

# Cloning and Co-Expression of Lipase and its Specific Foldase from *Ralstonia pickettii* BK6

Muhamad Azwar Syah<sup>1</sup>, Andreas Adhi Satya<sup>2</sup>, Esti Puspitasari<sup>2</sup>, Antonius Suwanto<sup>3\*</sup>, Nisa Rachmania Mubarik<sup>3</sup>

<sup>1</sup>Department of Biotechnology, Faculty of Mathematics and Natural Science, Halu Oleo University, Kendari, Indonesia

<sup>2</sup>Research and Development for Biotechnology, PT. Wilmar Benih Indonesia, Cikarang, Indonesia

<sup>3</sup>Department of Biology, Faculty of Mathematics and Natural Science, IPB University, Bogor, Indonesia

## ARTICLE INFO

### Article history:

Received April 18, 2022

Received in revised form July 6, 2022

Accepted July 12, 2022

### KEYWORDS:

Co-expression,

Foldase,

Lipase,

*Ralstonia pickettii*

## ABSTRACT

This study aimed to obtain a functional lipase (LipRM) from *Ralstonia pickettii* BK6 through a co-expression involving its foldase. The ORF of the LipRM was 999 bp while the gene encoding of lipase-specific foldase (LifRM) was 1,030 bp. LipRM and LifRM genes were cloned into a plasmid and were successfully co-expressed in *Escherichia coli* strains to produce functional LipRM. Enzyme activity from partially purified enzymes showed quite surprising results, LipRM activity in *E. coli* BL21 (DE3) was 25.84 U/ml, while the other strains (DH5α, HB101, S17-1λpir) were 628.98 U/ml, 761 U/ml, and 1206.46 U/ml, respectively. The highest relative activity of LipRM was found at 50-55°C and pH 7-8 with pNP-laurate (C<sub>12</sub>) as the preferred substrate specificity. LipRM activity was enhanced sharply in the presence of 30% organic solvents (methanol and ethanol) but decreased by more than 50% in the presence of detergents. This study was the first to report heterologous expression of *Ralstonia pickettii* lipase employing its native foldase resulting in functional lipase from subfamily I.2.

## 1. Introduction

Lipase (EC. 3.1.1.3) or triacylglycerol acyl-hydrolase is a hydrolase enzyme capable of hydrolyzing ester bonds in long-chain triacylglycerol to glycerol and fatty acids (Bharathi *et al.* 2019). Comprehensive studies of lipase over the past few years have unlocked a significant opportunity to utilize this enzyme for biotechnological applications. Due to the great variety of enzymatic properties and substrate specificities as well as the ease of isolation and production, bacterial lipases have been applied in detergent formulation, food, flavor industry, and catalyst for biodiesel (Bharathi *et al.* 2019; Jambulingan *et al.* 2019; Sasso *et al.* 2016; Yoo *et al.* 2011). Based on different amino acid homology and their biological component, bacterial lipase is classified into six subfamilies (Arpigny and Jaeger 1999).

Lipase from subfamily I.2 is of great interest to observe because this enzyme requires the help of a secondary protein called lipase-specific foldase or

chaperone for the correct folding and required for lipase secretion (Albayati *et al.* 2020; Putra *et al.* 2019; Viegas *et al.* 2020). In the absence of a chaperone, the resulting lipase will interpret as an inactive and insoluble enzyme. On the other hand, during lipase synthesis, approximately 30 different cellular proteins have to come together to form fully activated and involved 14 complex proteins for the secretion system (Albayati *et al.* 2020; Sandkvist 2001). Although this mechanism implies an inefficiency of enzyme production, lipases from subfamily I.2 show great potential for some applications.

As the pioneer of the lipase subfamily I.2, *Pseudomonas* and *Burkholderia* lipases have been widely used for industrial purposes such as detergent additives and various biotransformation. However, several bacterial lipases belonging to subfamily I.2 have not been explored extensively including *Ralstonia* lipase. Historically, these bacteria have tended to be associated with clinical issues, but in some cases, the secreted lipase enzyme has the advantage of being developed on an industrial scale because of its resistance to denaturation and inhibition of methanol (Quyen *et al.* 2005). Based on commercial enzymes in the biotechnology industry,

\* Corresponding Author

E-mail Address: asuwanto@apps.ipb.ac.id

recombinant lipase activity must be optimized to more than 15 U/mg to be applicable. Although the information is still limited regarding their lipase, several studies have increased the enzyme activity via cloning and co-expression to heterologous hosts. In fact, this approach faced many obstacles.

Quyen *et al.* (2005) have expressed *Ralstonia* lipase into *Escherichia coli* as a host cell by modifying the refolding system with *in vitro* interactions of chaperones outside the cell. Nevertheless, the enzyme is not feasible for industrial application, as it requires several hours to achieve the optimal activity. Co-expression of a lipase with two chaperones inserted into two different plasmids by *in vivo* refolding has been carried out as another approach to obtain functional lipases. This strategy causes the lipase to have low activity (Quyen *et al.* 2012). Inappropriate foldase or unsupported heterologous host could be the critical point for enhancing the lipase performance.

Several recent studies have demonstrated *Ralstonia* lipase, but none of them reported cloning and co-expression of lipase and its cognate foldase of *R. pickettii* BK6. Lipase activity of *Ralstonia* sp. NT80 only reaches 120 U/ml even though it has been induced by stearyl alcohol (Akanuma *et al.* 2013). *In vitro* refolding was able to increase lipase activity in *Ralstonia* sp. M1 (650 U/mg) with the use of chaperone ten times more than the quantity of lipase as the optimal ratio (Quyen *et al.* 2004). Our study uses a similar approach to that of Putra *et al.* (2019) by co-expressing subfamily I.2 lipases with their cognate foldases using single plasmid expression and *in vivo* refolding. This strategy was first performed on lipase and foldase coexpression of *R. pickettii* BK6 targeting functional lipases.

## 2. Materials and Methods

### 2.1. Samples and Reagents

*R. pickettii* BK6 was collected from PT. Wilmar Benih Indonesia (Syah 2022). Luria Bertani (1% peptone, 0.5% yeast extract, and 0.5% NaCl) was used for *E. coli* growth. *E. coli* DH5 $\alpha$  (Novagen, Germany), BL21 (DE3) pLyss (Invitrogen, USA), HB101, S17-1 $\lambda$ pir were used as the heterologous host, and pGEM-T Easy (Promega, USA) and pET-15by (Invitrogen, USA) as cloning and expression vector, respectively. Restriction enzymes (*NotI* and *NdeI*) and T4 ligase were purchased from NEB (USA).

### 2.2. Gene Amplification of Lipase and Foldase

Primers of RM\_LC\_Lip\_F (5'TCGGATAACGGAGGG CGATCG-3') and RM\_LC\_Lip\_R (5'-CTCATGGGAGTG CGTGATTG-3') were designed to amplify lipase (LipRM) and foldase (LifRM) genes simultaneously due to their contiguous location in the bacterial genome. Lipase sequences from the genus *Ralstonia* which are most closely related to *Ralstonia pickettii* BK6 were used as a reference in designing LipRM and LifRM primers. PCR reaction consists of pre-denaturation (94°C for 5 min), denaturation (94°C for 30 sec), primer annealing (60°C for 30 sec), extension (72°C for 2 min), and post-extension (72°C for 5 min) were performed for 30 cycles using PCR BIORAD C1000. LipRM and LifRM sequences were deposited into National Center for Biotechnology Information (NCBI) under accession number MH423623, and MH23624, respectively.

### 2.3. Phylogenetic and Modeling Analysis

Mega 6.06 software was used as a tool to reconstruct a phylogenetic tree of LipRM based on the maximum parsimony method which was compared to four families of bacterial lipase for reference. In addition, Swiss model, a bioinformatics web server, assisted by VMD application for lipase homology modeling.

### 2.4. Cloning and Co-expression of Lipase and Foldase Genes

The amplified lipase and foldase genes as an intact fragments were ligated into a cloning vector (pGEM-T Easy) using T4 ligase at 16°C for 16 hours. 20  $\mu$ l cloning vector (100 ng/ $\mu$ l) was used for transformation into 100  $\mu$ l *E. coli* DH5 $\alpha$  using the heat shock method at 42°C for 40 seconds and subsequently grown on Luria Agar (containing 100  $\mu$ g/ml ampicillin, 40  $\mu$ g/ml X-Gal, 0.1 mM IPTG, and supplemented with 0.5% TBN) at 37°C for 16 hours. The formation of a clear zone around the white colonies was indicated as a positive transformant and further verified by PCR using M13F and M13R primers.

pGEM-T Easy that containing lipase and foldase genes were digested with two restriction enzymes (*NotI* and *NdeI*) and ligated to the expression vector (pET-15by), which was further used for transformation into *E. coli* BL21 (DE3). The culture was grown on Luria Agar (containing 100 ng/ $\mu$ l ampicillin, 40 ng/ $\mu$ l, 40  $\mu$ g/ml X-Gal, 0.1 mM IPTG, and supplemented 0.5% TBN) at 37°C for 16 hours. The production of lipase was verified by the formation of a clear zone at the edge of the colony on the plate assay (Pulido *et al.* 2020).

## 2.5. Production of Recombinant LipRM and Partial Purification

Four different hosts (*E. coli* DH5 $\alpha$ , BL21 (DE3) pLyss, HB101, and S17-1 $\lambda$ pir) were involved to generate recombinant LipRM. The inoculum of each host was inoculated into 10 ml LB broth supplemented with the antibiotics selection, and grown at 37°C for 16 h and 200 rpm. 2% inoculum from these cultures was regenerated on 50 ml LB under the same conditions for 24 h, and when OD<sub>600</sub> achieved 0.6 (OD 1 = 5 x 10<sup>8</sup> cell/ml), it was induced with 50  $\mu$ l 0.5 mM IPTG.

In order to harvest the cells, the inoculum was centrifuged at 6000 xg for 10 min, the supernatant was discarded, and subsequently, pellets were resuspended with 5 ml 0.1 M Tris HCl-Buffer (pH 8.0). To expose the crude lipase, cells were disrupted using sonicator Handy Sonic for 15 min, and the supernatant solution was collected to obtain soluble expressed lipase. The soluble enzymes were partially purified with Amicon® Ultra 15 ml Centrifugal Filters (Merck, Germany) to remove small molecules or other proteins below 30 kDa.

## 2.6. Determination of Protein Molecular Weight

The molecular weight of the enzyme was determined using sodium dodecyl sulfate-polyacrylamide gel electrophoresis according to the modified Laemli method, involving 30% polyacrylamide and 10% SDS. After the enzymes migrated on the electrophoresis system, the gel plate was stained with Commasi Brilliant Blue. The protein bands were visualized by zymography analysis in LB agar supplemented with TCN. To remove staining residue, the gel portion containing the sample was immersed in 0.1 M HCl buffer (pH 8.0) and distilled water for 1 hour and 5 min, respectively. The spot of a clear zone on the sample well was aligned with the standard. The portion parallel to the marker protein was defined as the molecular weight of protein.

## 2.7. Lipase Assay

Lipase activity was measured spectrophotometrically using p-nitrophenyl laurate as a substrate according to the method of Martini *et al.* and Kim *et al.* with slight modification (Kim *et al.* 2012; Martini *et al.* 2014). In a general assay, the cocktail components for the hydrolysis reaction consisting of 940  $\mu$ l 0.1 M Tris HCl buffer (pH 8.0), 40  $\mu$ l cold ethanol absolute, 10

$\mu$ l crude enzyme, and 10  $\mu$ l pNP-ester substrate were sequentially mixed up. Subsequently, the component was immediately incubated at 50°C for 5 min, and absorbance was measured at 405 nm. Nitrophenol as standard was carried out according to the previous sample processing. Furthermore, one unit of lipase activity (U) was defined as the amount of enzyme required to liberate 1  $\mu$ mol pNP per minute. This assay was also used to measure the effect of temperature, pH, substrate specificity, metal ions, organic solvent, and detergents.

## 2.8. Characterization of Biochemical

The effect of temperature and pH on enzyme activity was observed based on the residual activity measured at 25–75°C and pH 3.0–10.0 using p-nitrophenyl laurate as the substrate (Arifin *et al.* 2013). The various 1 mM buffers involved in pH testing consisted of citrate buffer (pH 3.0), acetic buffer (pH 4.0), citrate-phosphate buffer (pH 5.0), phosphate buffer (pH 6.0–7.0), Tris-HCl buffer (pH 8.0–9.0), and glycine-NaOH buffer (pH 10.0).

Seven different substrates (pNP-butyrate/C<sub>2</sub>, pNP-hexanoate/C<sub>4</sub>, pNP-octanoate/C<sub>6</sub>, pNP-laurate/C<sub>8</sub>, pNP-myristate/C<sub>14</sub>, pNP-palmitate/C<sub>16</sub>, and pNP-stearate/C<sub>18</sub>) with varying carbon chain length, was used to assess the substrate specificity in lipase activity. Measurement of enzyme activity on substrate specificity was carried out at 50°C and pH 8.0.

Before determining the effect of various metal ions and chelating agents, organic solvents, and detergents, the enzymes were mixed with each treatment, then preincubated at 30°C for 30 min. Metal ions and chelating agent tested in this study consisted of Fe<sup>2+</sup>, Cu<sup>2+</sup>, Mg<sup>2+</sup>, Ca<sup>2+</sup>, Zn<sup>2+</sup>, Na<sup>+</sup>, Mn<sup>+</sup>, K<sup>+</sup>, and EDTA); the effect of 10% and 30% organic solvent (methanol, ethanol, 2-propanol, 1-butanol, and *n*-hexane), as well as 1% and 5% detergents (SDS, triton X-100, tween-20, and tween-80) were also tested. Residual activity was measured at 50°C and pH 8.0 involving pNP-laurate as a substrate (Quyen *et al.* 2005).

## 3. Results

### 3.1. Lipase and Foldase Sequence of BK6

The interpretation of the BK6 lipase and foldase genes are contiguous in the conformation of the

bacterial genome of BK6, which is separated by 37 bp short sequences termed the intergenic region. Moreover, both enzymes were controlled by only a single promoter located upstream of the lipase genes (Figure 1). For this study, the BK6 lipase is denoted by LipRM, while the foldase is LifRM. The open reading frame (ORF) of the lipRM gene was 999 bp which will undergo translation to form a complete lipase consisting of 333 amino acids. Meanwhile, 43 residues upstream of all these amino acids were annotated as the removable signal peptide which assisted lipase to migrate into the periplasmic side via the inner membrane protein. Prior to transport through the channel, a protease protein cleaves off the signal sequence from lipase that has been recognized by Sec protein. Therefore, the resulted mature lipase has a molecular weight of approximately 30 kDa (Figure 2).

The gene encoding LifRM was slightly different from lipase, in that the gene consists of 1,030 bp of nucleotides that made up 350 amino acids. The initial 26 residues represent the signal peptide with identical function like previously described. Then, based on amino acid alignment, it was shown that LipRM had 97% similarity with a lipase of *R. pickettii* (GenBank: KFL21962.1), while LifRM was 99% similar to the lipase specific chaperone from *R. pickettii* (GenBank: WP102064761.1).

### 3.2. Phylogenetic and Modelling of Lipase

Four families of bacterial lipase obtained from the NCBI database were utilized as references to construct the phylogenetic relationship between LipRM-BK6 and the references. The cluster pattern disclosed that the LipRM-BK6 was in the same group as other lipase subfamilies I.2 and was identified as a monoclade with lipase from *R. pickettii* (KFL21962.1). Drawing an inference from the phylogenetic tree, it is proposed that LipRM-BK6 belongs to the lipase subfamily I.2 (Figure 3).

The motif of eight  $\beta$  sheets flanked by nine  $\alpha$ -helices was discovered as the output of homology modeling from LipRM-BK6 (Figure 4A). The

conserved pentapeptide region and triad catalytic of this lipase were amino acids of Gly-His-Ser-Gln-Gly at residue 124-128 and His<sup>298</sup>-Ser<sup>126</sup>-Asp<sup>276</sup> respectively, which accommodate the establishment of active conformation (Figure 4B). Moreover, the presence of a short  $\alpha$  helix at the protein surface which covered the active site of this lipase was detected (Figure 4C). The last important feature of the LipRM-BK6 structure has a disulfide bridge (Figure 4D).

### 3.3. Co-expression of Recombinant LipRM

The success of recombinant LipRM co-expressed with LifRM can be observed through qualitative parameters based on the formation of clear zones on a selective medium. The results showed that this approach successfully expressed functional LipRM

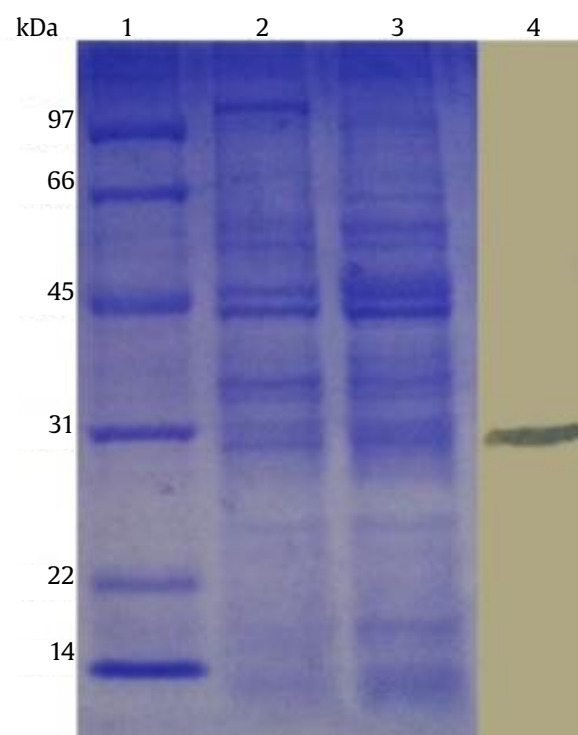


Figure 2. SDS-PAGE and zymogram analysis of LipRM. Lane 1, protein marker; 2, crude enzyme (1 mg); 3, partially purified enzyme (1 mg); 4, zymogram in LB agar containing 0.5% TCN

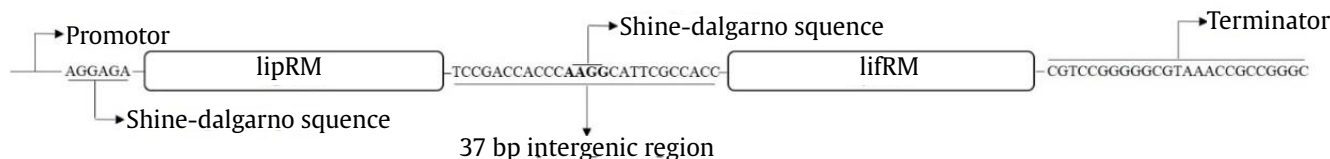


Figure 1. Representation the operon structure of lipRM and lifRM

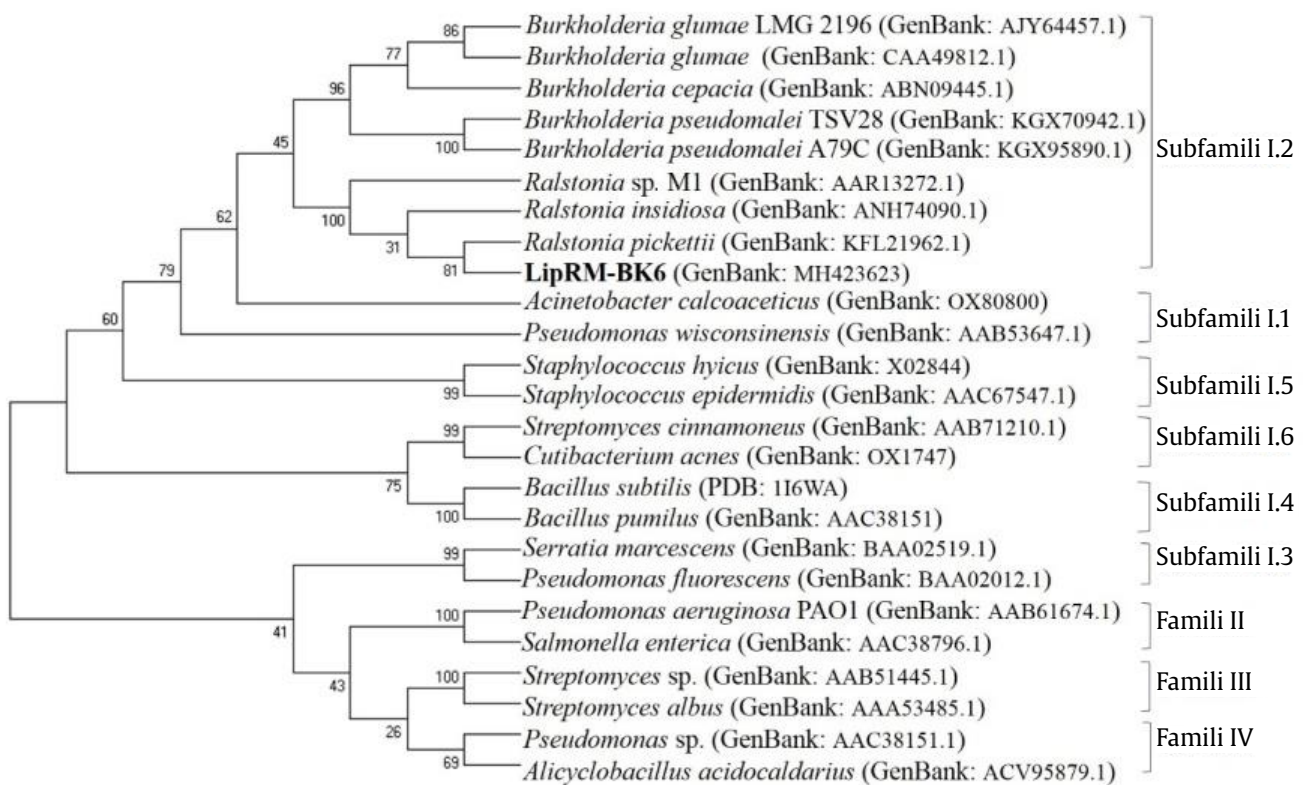


Figure 3. Phylogenetic tree of *LipRM* with four lipolytic enzyme families as references based on maximum parsimony employing 1000x bootstrap

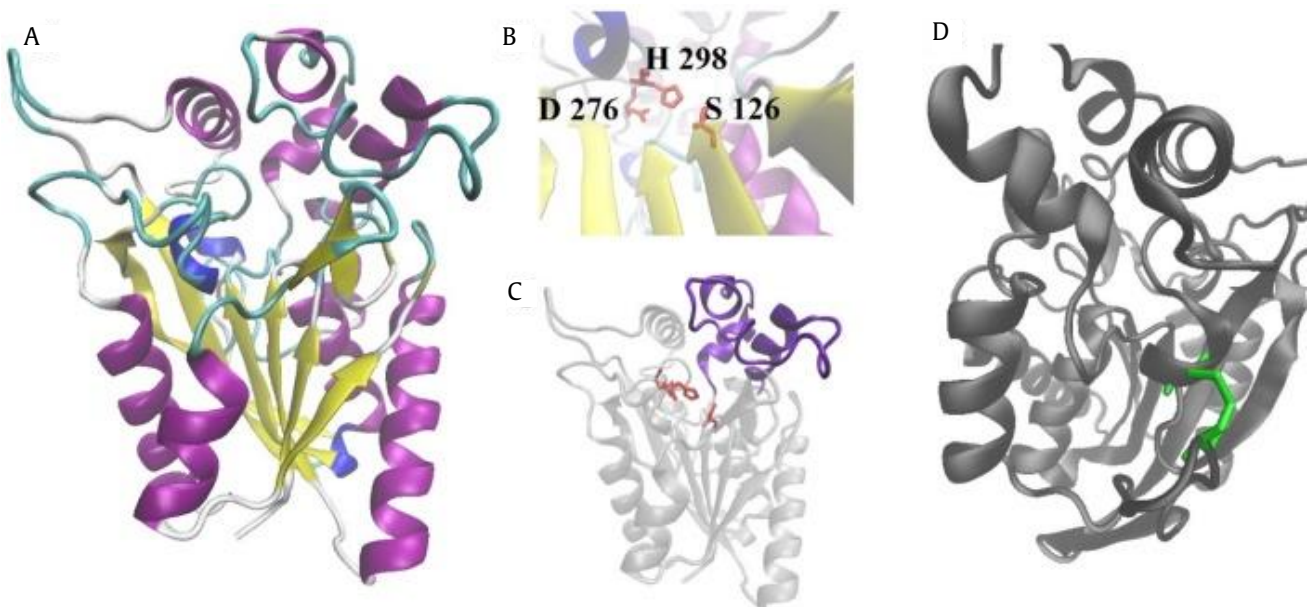


Figure 4.  $\alpha/\beta$  hydrolase structure of *LipRM*. (A) Three-dimensional structure, (B) catalytic triad sites (the red stick), (C) short  $\alpha$  helix covered the active site (the blue), (D) two-cysteins formed a disulfide bridge (the green structure)

which was verified by the appearance of a clear zone around the cell colony on TBN-supplemented LB media (Figure 5). All heterologous hosts (DH5 $\alpha$ , HB101, S17-1 $\lambda$ pir, and BL21 (DE3) pLyss) displayed clear zones on selective media indicating fully activated recombinant LipRM.

To determine the efficiency of the co-expression system, both genes were cloned using two different plasmids (pGEM-T Easy and pET-15by) and involving four different *E. coli* strains (DH5 $\alpha$ , HB101, S17-1 $\lambda$ pir, and BL21 (DE3) pLyss) as heterologous hosts. LipRM and LifRM genes were cloned into an expression vector (pET-15by) and cloning vector (pGEM-T Easy) to compare the enzyme activity among the two vectors. The vector of pET-15by was used for transformation into *E. coli* BL21 (DE3), while pGEM-T Easy was transformed into 3 different strains DH5 $\alpha$ , HB101, S17-1 $\lambda$ pir. The measurement of enzyme activity after partially purified showed quite surprising results, LipRM activity in *E. coli* BL21 (DE3) was 25.84 U/ml, while the other strains

(DH5 $\alpha$ , HB101, S17-1 $\lambda$ pir) were significantly higher with enzyme activity of 628.98 U/ml, 761 U/ml, and 1206.46 U/ml, respectively.

### 3.4. Biochemical Characterization

#### 3.4.1. Effect of Temperature on LipRM Activity

All the parameters of biochemical testing using the recombinant lipase of LipRM. To determine the optimal temperature of LipRM, the enzyme activity was assayed at temperatures ranging from 25 to 75°C and incubated for 5 min. The highest relative activity of LipRM was found at 50-55°C. However, treatments at 25°C and 75°C showed a significant reduction of up to 70% of the LipRM activity (Figure 6A). Since the optimum activity was displayed at 50-55°C, this enzyme was classified as a thermostable enzyme.

#### 3.4.2. Effect of pH on LipRM Activity

The result of testing the relative activity of LipRM to various pH ranging from pH 3 to pH 10 showed that the enzyme activity was significantly different when hydrolyzing the substrate at pH less than 7 and pH more than 7. The LipRM enzyme still maintained its activity an average of 80% after treatment at pH 7-10. However, the best preference for achieving the optimal function of this enzyme was found at pH 7.0-8.0 because the activity of LipRM remained more than 95% after treatment at pH 7-8 (Figure 6B). Incubation of the enzyme at pH 3-6 is not recommended because it removed LipRM activity by up to 75%. Therefore, based on the data, LipRM was categorized as an alkaline-tolerant enzyme.

#### 3.4.3. Substrate Specificity of LipRM

Determination of substrate specificity was carried out using various substrates with different acyl chain lengths at optimum temperature and pH.



Figure 5. Colonies with clear zones as positive transformants

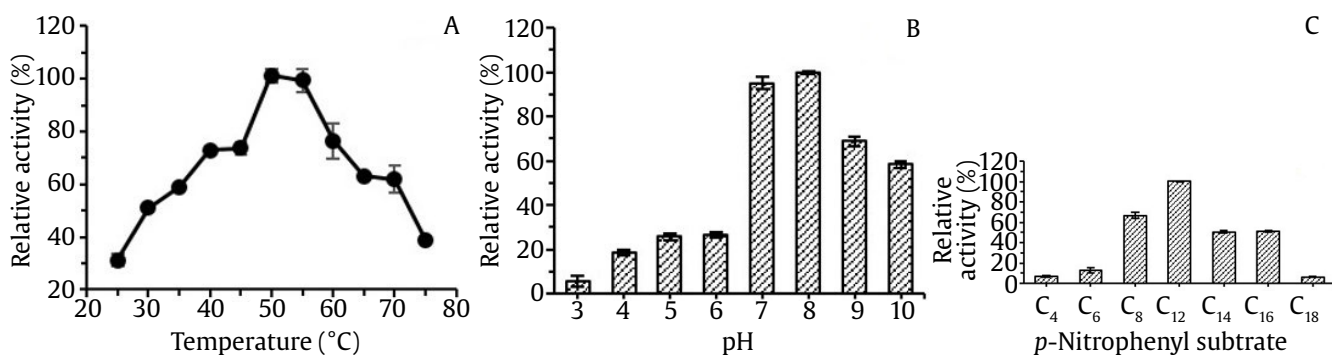


Figure 6. Biochemical characteristics of LipRM. (A) Effect of temperature, (B) effect of various pH, (C) substrate specificity of LipRM on different length of fatty acids

The maximum activity of the enzyme was achieved when the LipRM hydrolyzed the pNP-laurate ( $C_{12}$ ) compared to other substrates used in this study. However, outside of this substrate, activity rapidly dropped down to around 50% on some substrates such as pNP-laurate ( $C_8$ ), pNP-myristate ( $C_{14}$ ), and pNP-palmitate ( $C_{16}$ ), and up to more than 80% at  $C_4$ ,  $C_6$  as well as  $C_{18}$  (Figure 6C). Based on these data indicate that the hydrolysis ability of LipRM tends to be supported by the substrate specificity which is rich in lauric fatty acid.

#### 3.4.4. Effect of Metal Ions on LipRM Activity

The effect of metal ions on the activity of LipRM-BK6 displayed that the treatments of  $Fe^{2+}$ ,  $Cu^{2+}$ ,  $Mg^{2+}$ ,  $Ca^{2+}$ ,  $Na^+$ ,  $Mn^+$ , and  $Zn^{2+}$  at 1 mM final concentration impacted enormously enzyme activity by decreasing the enzyme ability to hydrolyze substrate, and no activity was detected in the presence of  $Mn^+$  and  $Zn^{2+}$  (Table 1).

#### 3.4.5. Effect of Various Organic Solvents on LipRM Activity

One of the critical factors influencing the application of lipase in industrial processes is the stability of enzymes in organic solvents. For this study, two different concentrations (10% and 30%) were used to observe the effect of various organic solvents on LipRM Activity. Interestingly, the enzyme activity of LipRM enhanced sharply in the presence of 30% organic solvents including methanol, ethanol, 2-propanol, 1-butanol, and *n*-hexane compared to 10% organic solvents. At 10% organic solvents such as 2-propanol, 1-butanol, and *n*-hexane increased the LipRM activity which exceeded the control activity, but methanol and ethanol decreased the residual activity up to  $62.0\pm11.3$  and  $69.4\pm9.7$ , respectively (Table 2).

#### 3.4.6. Effect of Various Detergents on LipRM Activity

The hydrolytic activity of LipRM was significantly reduced by more than 50% after being treated with detergents such as Triton X-100, tween-20, and tween-80 at concentrations of 1% and 5%, respectively, and was quite stable at 1% SDS still retaining its activity up to  $95.7\pm7.3$  (Table 3).

Table 1. Effect of metal ions on LipRM activity

Metal ion and chelating	Relative activity (%)
Control	$100.3\pm0.7$
KCl	$55.0\pm1.0$
FeCl <sub>2</sub>	$34.2\pm0.4$
CuCl <sub>2</sub>	$30.4\pm3.1$
MgCl <sub>2</sub>	$23.6\pm7.1$
CaCl <sub>2</sub>	$39.2\pm7.6$
NaCl	$11.4\pm5.3$
MnSO <sub>4</sub>	Undetected
ZnCl <sub>2</sub>	Undetected
EDTA	$50.0\pm2.9$

Table 2. Effect of organic solvents on LipRM activity

Organic solvent	Relative activity (%)	
	10%	30%
Control	$100.0\pm2.1$	$100.0\pm5.1$
Methanol	$62.0\pm11.3$	$147.6\pm10.3$
Ethanol	$69.4\pm9.7$	$352.8\pm12.2$
2-propanol	$142.9\pm7.3$	$431.8\pm15.0$
1-butanol	$453.5\pm14.3$	$481.6\pm15.6$
<i>n</i> -hexane	$355.7\pm17.4$	$410.1\pm3.8$

Table 3. Effect of various detergents on LipRM activity

Detergent	Relative activity (%)	
	1%	5%
Control	$100.0\pm0.5$	-
Triton X-100	$17.5\pm6.7$	Undetected
Tween-20	$8.5\pm3.5$	$49.7\pm1.2$
Tween-80	$21.6\pm6.5$	$7.8\pm0.5$
SDS	$95.7\pm7.3$	Undetected

## 4. Discussion

The absence of a promoter in the foldase gene reflects that the enzyme function is dependent on the lipase expression, and carries out its performance within the framework of the operon system (Kranen *et al.* 2014). However, Shine-Dalgarno sequences are present at the initiation side of both the lipase and foldase, as it is important for initiating protein synthesis (Nowroozi *et al.* 2014; Oesterle *et al.* 2017; Omotajo *et al.* 2015).

The three-dimensional structure of the  $\beta$ -sheet flanked by  $\alpha$ -helices is a particular feature shared by bacterial lipase, although the enzyme was found to be very diverse (Khan *et al.* 2017; Putra *et al.* 2019). The presence of a short helix on the surface of the protein covering the active site of LipRM-BK6 correlates with the open and closed conformation during substrate

interaction (Masomian *et al.* 2016). Moreover, the disulfide bridge structure in LipRM-BK6 plays a role in maintaining the stability and conformation of the protein (Pulido *et al.* 2020).

Broadly speaking, the main parameter that characterizes the lipase I.2 subfamily lies in its molecular size of 33 kDa which forms antiparallel double  $\beta$ -strands on the protein surface and has a conserved pentapeptide with the residue Gly-Xaa-Ser-Xaa-Gly. In addition, to support their physiological functions, lipase from subfamily I.2 depends on a protein chaperone named lipase specific foldase for refolding. Based on molecular analysis and phylogenetic construction, LipRM is feasible to be proposed as a subfamily of I.2 lipases which has a conserved pentapeptide in the form of Gly-His-Ser-Gln-Gly at residue 124-128.

Because LipRM was classified into lipase subfamily I.2, a specific strategy was needed to express this lipase into a functional form. Our study employed a novel approach in which LipRM was co-expressed with the cognate foldase (LifRM), and simultaneously ligated in the same plasmid so that the protein refolding occurred naturally in the host cell. Interestingly, this approach displayed that the LipRM was completely activated. A comprehensive study a few years ago has proved that the lipase subfamily I.2 absolutely was dependent on the existence of foldase protein to get the functional lipase. Moreover, An appropriate foldase is one of the main factors that support the activation process. Foldase, also known as chaperone, is a protein that assisted the refolding conformational to create the biological function in this lipase (Albayati *et al.* 2020; Kranen *et al.* 2014).

Our study can address some of the challenges currently being faced in producing active *Ralstonia* lipase. Several approaches have been carried out, including modification of refolding system and involving two different foldases, but this method was still not effective enough to produce functional lipases of subfamily I.2 (Quyen *et al.* 2012). In recent years, the recombinant enzyme approach to improve the production of lipase in large amounts employing *E. coli* has become very popular. However, in many cases, the inclusion body and low-level expression were the obstacles frequently encountered in the recombinant lipase.

Basically, to produce the recombinant lipase, the most widely used are *E. coli* BL21 (DE3) and

expression vectors such as pET-15by because they have the ability to produce high amounts of protein. However, this case was uncorrelated to our study which displayed that DH5 $\alpha$ , HB101, S17-1 $\lambda$ pir was potential references as co-expression host to produce recombinant LipRM compared to BL21 (DE3). One of the main factors that caused the S17-1 $\lambda$ pir strain to have the highest enzyme activity because this strain was genetically modified to contain the RecA mutant allele so as to ensure the stability of the inserted plasmid.

We have not found a scientific reason from previous studies that can reveal the cause of recombinant LipRM production carried out by DH5 $\alpha$ , HB101, S17-1 $\lambda$ pir better than BL21 (DE3). However, this can be expected due to the difference in the use of promoters in the two vectors. pET-15by was controlled by the inducible promoter (T7), whereas LipRM on pGEM-T Easy was a constitutive promoter (SP6). SP6 polymerase consistently produces higher yields of RNA than T7 polymerase (Stump and Hall 1993).

The biochemical characterization of LipRM plays an important role in the application of enzymes in the biotechnology industry. LipRM stability at 50-55°C and pH 7.0-8.0 can support the use of this enzyme in biodiesel production, detergent formulation, and biotransformation (Lu *et al.* 2012; Yoo *et al.* 2011). The substrate specificity of LipRM is quite different from other *Ralstonia* lipases which tend to be specific for C<sub>8</sub> and C<sub>16</sub> ester substrates. One of the scientific reasons for this difference is that the LipRM active site has a unique geometric that only recognizes a substrate that fits that shape (Latip *et al.* 2016).

LipRM activity tends to be inhibited by the presence of metal ions (Fe<sup>2+</sup>, Cu<sup>2+</sup>, Mg<sup>2+</sup>, Ca<sup>2+</sup>, Na<sup>+</sup>, Mn<sup>+</sup>, and Zn<sup>2+</sup> at 1 mM final concentration) on the substrate. Basically, metal ions can act as cofactors that help in increasing enzyme activity because they can stabilize the negative charge during the interaction between the substrate and the enzyme. However, metal ions can increase the energy barrier that can inhibit enzyme activity (Paul and Mishra 2021). Previous studies also showed that the *Ralstonia* lipase was inhibited by the presence of metal ions such as Cu<sup>2+</sup>, Mg<sup>2+</sup>, Fe<sup>2+</sup>, and Zn<sup>2+</sup> on the substrate (Lu *et al.* 2012; Quyen *et al.* 2005).

Our study showed a significant increase in LipRM activity up to about 4 times higher than normal due to the addition of 30% organic solvents (ethanol,

methanol, 1-butanol, 2-propanol, and *n*-hexane) to the substrate. The polarity-hydrophobicity (log P-value) is one of the main keys that affect enzyme activity in the presence of organic solvents in the substrate (Mayorov *et al.* 2019). The highest LipRM activity was found in 1-butanol ( $C_4$ ) and *n*-hexane ( $C_6$ ) because the amount of carbon in both organic solvents was higher than in ethanol, methanol, and propanol which correlated with an increase in the hydrophobicity ratio. Organic solvents can increase the hydrophobicity of the  $\alpha$ -helix structure of the lipase which has implications for supporting the interaction between the substrate and the active site of the enzyme. LipRM stability to ethanol and methanol plays an important role in biodiesel production through a transesterification reaction (Adina *et al.* 2021; Jayaraman *et al.* 2020).

LipRM-BK6 was more stable to 1% SDS detergent compared to some of the previously reported *Ralstonia* lipases (Yoo *et al.* 2011). SDS is an anionic surfactant that has 12 carbon atoms in its tail and is an important component in many commercial detergents. Detergents increase the hydrophobicity of the environment, resulting in changes in the tertiary structure of proteins (Fatima *et al.* 2014). The stability of alkaline lipases to detergents is useful as an additive component in detergent formulations.

## Acknowledgements

This work was funded by Research and Development for Biotechnology, PT. Wilmar Benih Indonesia, Cikarang, Indonesia.

## References

- Adina, S.R., Suwanto, A., Meryandini, A., Puspitasari, E., 2021. Expression of novel acidic lipase from *Micrococcus luteus* in *Pichia pastoris* and its application in transesterification. *J Gen Eng and Biotechnol.* 19, 55-66. <https://doi.org/10.1186/s43141-021-00155-w>
- Akanuma, G., Ishibashi, H., Miyagawa, T., Yoshizawa, R., Watanabe, S., Shiwa, Y., Yoshikawa, H., Ushio, K., Ishizuka, M., 2013. EliA facilitates the induction of lipase expression by stearyl alcohol in *Ralstonia* sp. NT80. *Fems Microbiol Lett.* 339, 48-56. <https://doi.org/10.1111/1574-6968.12055>
- Albayati, S.H., Masomian, M., Ishak, S.N.M., Ali, M.S., Thean, A.L., Shariff, F., Noor, N.D., Rahman, R.N.Z., 2020. Main structural targets for engineering lipase substrate specificity. *Catalysts.* 10, 1-34. <https://doi.org/10.3390/catal10070747>
- Arifin, Ranlym, A., Kim, S.J., Yim, J.H., Suwanto, A., Kim, H.K., 2013. Isolation and biochemical characterization of *Bacillus pumilus* lipases from the Antarctic. *J Microbiol Biotechnol.* 23, 661-667. <https://doi.org/10.4014/jmb.1212.12040>
- Arpigny, J.L., Jaeger, K.E., 1999. Bacterial lipolytic enzyme: classification and properties. *Biochem J.* 343, 177-183.
- Bharathi, D., Rajalakshmi, G., Komathi, S., 2019. Optimazation and production of lipase enzyme from bacterial strains isolated from petrol spilled soil. *Journal of King Saud University.* 31, 898-901. <https://doi.org/10.1016/j.jksus.2017.12.018>
- Fatima, S., Ajmal, R., Badr, G., Khan, R.W., 2014. Harmful effect of detergent on lipase. *Cell Biochem Biophys.* 70, 59-763. <https://doi.org/10.1007/s12013-014-9978-4>
- Jambulingan, R., Shalma, M., Shankar, V., 2019. Biodiesel production using lipase immobilized functionalized magnetic nanocatalyst from oleaginous fungal lipid. *Journal of Cleaner Production.* 215, 245-258. <https://doi.org/10.1016/j.jclepro.2018.12.146>
- Jayaraman, J., Alagu, K., Appavu, P., Joy, N., Jayaram, P., Mariadoss, A., 2020. Enzymatic production of biodiesel using lipase catalyst and testing of an unmodified compression ignition engine using its blends with diesel. *Renewable Energy.* 145, 399-407. <https://doi.org/10.1016/j.renene.2019.06.061>
- Khan, F.I., Lan, D., Durrani, R., Huan, W., Zhao, Z., Wang, Y., 2017. The lid domain in lipases: structural and functional determinant of enzymatic properties. *Front Bioeng. Biotechnol.* 5, 1-13. <https://doi.org/10.3389/fbioe.2017.00016>
- Kim, Y.O., Khosasih, V., Nam, B.H., Lee, S.J., Suwanto, A., Kim, H.K., 2012. Gene cloning and catalytic characterization of cold adapted lipase of *Photobacterium* sp. MA1-3 isolated from blood clam. *J Biosci Bioeng.* 144, 589-595. <https://doi.org/10.1016/j.jbbiosc.2012.06.013>
- Kranen, E., Detzel, C., Weber, T., Jose, J., 2014. Autodisplay for the co-expression of lipase and foldase on the surface of *E. coli*: washing with designer bugs. *Microb Cell Fact.* 13, 1-12.
- Latip, W., Rahman, R.N.Z.R.A., Leow, A.T.C., Shariff, F.M., Ali, M.S.M., 2016. Expression and characterization of thermotolerant lipase with broad pH profiles isolated from an Antarctic *Pseudomonas* sp. strain AMS3. *PeerJ.* 4, 1-20. <https://doi.org/10.7717/peerj.2420>
- Lu, J., Brigham, C.J., Rha, C., Sinskey, A.J., 2012. Characterization of an extracellular lipase and its chaperon from *Ralstonia eutropha* H16. *Appl Microbiol Biotechnol.* 97, 2443-2454. <https://doi.org/10.1007/s00253-012-4115-z>
- Martini, V.P., Glogauer, A., Muller-Santos, M., Lule, J., Souza, E.M., Mitchell, D.A., Pedrosa, F.O., Krieger, N., 2014. First co-expression of a lipase and its specific foldase obtained by metagenomics. *Microb Cell Fact.* 13, 171-184. <https://doi.org/10.1186/s12934-014-0171-7>
- Masomian, M., Rahman, R.N.Z.R.A., Saleh, A.B., Basri, M., 2016. Analysis of comparative sequence and genomic data to verify phylogenetic relationship and explore a new subfamily of bacterial lipases. *PLOS One.* 11, 1-20. <https://doi.org/10.1371/journal.pone.0149851>
- Mayorov, A., Peraro, M.D., Abriata, L.A., 2019. Active site-induced evolutionary constraints follow fold polarity principles in soluble globular enzymes. *Molecular Biology and Evolution.* 36, 1728-1733. <https://doi.org/10.1093/molbev/msz096>
- Nowroozi, F.F., Baidoo, E.E.K., Ermakov, S., Redding-Johanson, A.M., Batth, T.S., Petzold, C.J., Keasling, J.D., 2014. Metabolic pathway optimization using ribosome binding site variants and combinatorial gene assembly. *Appl Microbiol Biotechnol.* 98, 1567-1581. <https://doi.org/10.1007/s00253-013-5361-4>
- Oesterle, S., Genggross, D., Schmitt, S., Roberts, T.M., Panke, S., 2017. Efficient engineering of chromosomal ribosome binding site libraries in mismatch repair proficient *Escherichia coli*. *Scie Reports.* 7, 1-10. <https://doi.org/10.1038/s41598-017-12395-3>

- Omotajo, D., Tate, T., Cho, H., Choudhary, M., 2015. Distribution and diversity of ribosome binding sites in prokaryotic genomes. *BMC Genom.* 16, 604-611. <https://doi.org/10.1186/s12864-015-1808-6>
- Paul, A., Mishra, S., 2021. Metal-ion promiscuity of microbial enzyme DapE at its second metal-binding site. *J Biol Inorg Chem.* 26, 569-582. <https://doi.org/10.1007/s00775-021-01875-7>
- Pulido, I.Y., Prieto, E., Pieffet, G.P., Mendez, L., Jimenez-Junca, C.A., 2020. Functional heterologous expression of mature lipase LipA from *Pseudomonas aeruginosa* PSA01 in *Escherichia coli* Shuffle and BL21 (DE3): effect of the expression host on thermal stability and solvent tolerance of the enzyme produced. *Int J Mol Sci.* 22, 3925-3944. <https://doi.org/10.3390/ijms21113925>
- Putra, L., Natadiputri, G.H., Meryandini, A., Suwanto, A., 2019. Isolation, cloning and co-expression of lipase and foldase genes of *Burkholderia territorii* GP3 from Mount Papandayan Soil. *J Microbiol and Biotechnol.* 29, 944-951. <https://doi.org/10.4014/jmb.1812.12013>
- Quyen, D.T., Nguyen, T.T., Le, T.T.G., Kim, H.K., Oh, T.K., Lee, J.K., 2004. A novel lipase/chaperone pair from *Ralstonia* sp. M1: analysis of the folding interaction and evidence for gene loss in *R. solanacearum*. *Mol Gen Genomics.* 272, 538-549. <https://doi.org/10.1007/s00438-004-1084-7>
- Quyen, D.T., Lee, T.T.G., Nguyen, T.T., Oh, T.K., Lee, J.K., 2005. High-level heterologous expression and properties of a novel lipase from *Ralstonia* sp. M1. *Protein Expr Purif.* 39, 97-106. <https://doi.org/10.1016/j.pep.2004.10.001>
- Quyen, D.T., Vu, C.H., Le, G.T.T., 2012. Enhancing functional production of a chaperone-dependent lipase in *Escherichia coli* using the dual expression cassette plasmid. *Microb Cell Fact.* 11, 1-12.
- Sandkvist, M., 2001. Micro-review biology of type II secretion. *Mol Microbiol.* 40, 271-283.
- Sasso, F., Natalello, A., Castoldi, S., Lotti, M., Santambrogio, C., Grandori, R., 2016. *Burkholderia cepacia* lipase is a promising biocatalyst for biofuel production. *Biotechnol J.* 11, 1-6. <https://doi.org/10.1002/biot.201500305>
- Stump, W.T., Hall, K.B., 1993. SP6 RNA polymerase efficiently synthesizes RNA from short double-stranded DNA templates. *Nucleic Acid Res.* 21, 5480-5484. <https://doi.org/10.1093/nar/21.23.5480>
- Syah, M.A. 2022. Isolation and molecular characterization of lipolytic bacterial 16S rRNA gene from cashew nutshell waste. *Jurnal Sumberdaya Hayati* 8, 20-26. <https://doi.org/10.29244/jsdh.8.1.20-26>
- Viegas, A., Dollinger, P., Verma, N., Kubiak, J., Viennet, T., Seidel, C.A.M., Gohlke, H., Etzkorn, M., Kovacic, F., Jaeger, K.E., 2020. Structural and dynamic insights revealing how lipase binding domain MD1 of *Pseudomonas aeruginosa* foldase affects lipase activation. *Scie Report.* 10, 1-15. <https://doi.org/10.1038/s41598-020-60093-4>
- Yoo, H.Y., Simkhada, J.R., Cho, S.S., Park, D.H., Kim, S.W., Seong, C.N., Yoo, J.C., 2011. A novel alkaline lipase from *Ralstonia* with potential application in biodiesel production. *Bioresour Technol.* 102, 6104-6111. <https://doi.org/10.1016/j.biortech.2011.01.046>